



HAL
open science

Neuroprotective Activities of New Monoterpenoid Indole Alkaloid from *Nauclea officinalis*

Sook Yee Liew, Wen Qi Mak, Hin Yee Thew, Kooi Yeong Khaw, Hazrina Hazni, Marc Litaudon, Khalijah Awang

► **To cite this version:**

Sook Yee Liew, Wen Qi Mak, Hin Yee Thew, Kooi Yeong Khaw, Hazrina Hazni, et al.. Neuroprotective Activities of New Monoterpenoid Indole Alkaloid from *Nauclea officinalis*. *Processes*, 2023, 11 (3), pp.646. 10.3390/pr11030646 . hal-04127288

HAL Id: hal-04127288

<https://hal.science/hal-04127288v1>

Submitted on 13 Jun 2023

HAL is a multi-disciplinary open access archive for the deposit and dissemination of scientific research documents, whether they are published or not. The documents may come from teaching and research institutions in France or abroad, or from public or private research centers.

L'archive ouverte pluridisciplinaire **HAL**, est destinée au dépôt et à la diffusion de documents scientifiques de niveau recherche, publiés ou non, émanant des établissements d'enseignement et de recherche français ou étrangers, des laboratoires publics ou privés.

Neuroprotective activities of new monoterpenoid indole alkaloid from *Nauclea officinalis*

Sook Yee Liew^{1,2,*}, Mak Wen Qi³, Thew Hin Yee³, Kooi Yeong Khaw^{3,*}, Hazrina Hazni², Marc Litaudon⁴, Khalijah Awang^{2,5}

¹ Chemistry Division, Centre for Foundation Studies in Science, Universiti Malaya, 50603 Kuala Lumpur, Malaysia.

² Centre for Natural Products Research and Drug Discovery (CENAR), Universiti Malaya, 50603 Kuala Lumpur, Malaysia.

³ School of Pharmacy, Monash University Malaysia, 47500 Bandar Sunway, Selangor, Malaysia.

⁴ Institut de Chimie des Substances Naturelles, CNRS-ICSN UPR2301, University Paris-Saclay, 91198 Gif-sur-Yvette Cedex, France

⁵ Department of Chemistry, Faculty of Science, Universiti Malaya, 50603 Kuala Lumpur, Malaysia.

*Corresponding author. Tel.: +603-79675927; +603-55146135

E-mail address: joeyliew5382@um.edu.my; khaw.kooiyeong@monash.edu

Abstract: Phytochemical investigation on the bark of *Nauclea officinalis* led to the isolation of a new monoterpenoid indole alkaloid, naucediol. The structure of the compound was identified through extensive spectroscopic analysis. Naucediol displayed cholinesterase inhibitory activities towards TcAChE and hBChE with IC₅₀ values of 15.429 and 8.756 μM, respectively. The mode of inhibition of naucediol was mixed-type inhibition and the Ki value is correlated with the IC₅₀ value in which naucediol exhibited higher butyrylcholinesterase inhibition activity. Molecular docking revealed that naucediol interacts with the choline-binding site and the catalytic triad of TcAChE and hBChE. This study also demonstrated the neuroprotective potential of naucediol against amyloid beta-induced cytotoxicity and LPS-induced neuroinflammation activity in a dose-dependent manner.

Keywords: *Nauclea officinalis*, indole alkaloids, amyloid beta, neuroinflammation, cholinesterase

Citation: To be added by editorial staff during production.

Academic Editor: Firstname Last-name

Received: date

Revised: date

Accepted: date

Published: date



Copyright: © 2022 by the authors. Submitted for possible open access publication under the terms and conditions of the Creative Commons Attribution (CC BY) license (<https://creativecommons.org/licenses/by/4.0/>).

1. Introduction

Alzheimer's disease (AD) is the most common type of dementia and it is estimated to affect 131 million people globally by the year 2050. Over the years, several hypotheses have been proposed to slow down the progression of AD including by improving type 2 diabetes mellitus [1] and the discovery of next-generation therapeutics for the management of AD. It includes cholinesterase, β-amyloid, tau, and neuroinflammation hypotheses. However, current drugs available to slow down the progression of AD are cholinesterase inhibitors (Donepezil, Rivastigmine, and Galantamine) and Memantine (NMDA antagonist), however, they are associated with limitations such as adverse effects, low bioavailability, and inconsistent efficacy [2]. These drugs are based on a one-drug-one target hypothesis whilst the etiology of AD is multifactorial [3]. Therefore, this necessitates the need for novel agents with multi-targeted potential. Natural products are of particular interest due to their ability to reduce oxidative stress, and anti-inflammation

and could potentially slow down the progression of AD [4,5]. This further reinforces the possibility of discovering new agents from natural derivatives.

Natural products also are known as secondary phytometabolites. These organic chemicals do not directly affect cell growth and proliferation, but they enhance survival mechanisms in living organisms [6]. Investigations in molecular mechanisms and docking analysis, have shed light on molecular activities of these secondary phytometabolites [7]. Most secondary phytometabolites are known to interfere with inflammatory mediators such as cytokines and peptides and inhibit macrophage activity [8] in which indole alkaloids; topsentins and dragmacidins [9] are some good examples. *Nauclea officinalis* (Pierre ex Pitard) Merr. & Chun, a traditional Chinese medicine from the Rubiaceae family, is widely used to treat exogenous fever, pink eye, pneumonia and acute jaundice in China. It has anti-inflammatory and anti-malarial properties [10-12]. In addition, *Nauclea officinalis* has been known to contain many indole alkaloids with biological activities. For example, 17-oxo-19-(Z)-naucline and naucleoffeine H displayed anti-inflammatory effects by decreasing the LPS-stimulated production of nitric oxide in RAW264.7 cell [13,14]. Hence, in continuous search for bioactive indole alkaloids from Rubiaceae family [15-17], a new monoterpene indole alkaloid, nauclediol has been isolated from *Nauclea officinalis*. In the present study, the isolation and structural elucidation of the nauclediol is reported together with the neuroprotective potential of the compound.

2. Materials and Methods

2.1. General Procedures

The general procedures were the same as previously described [18].

2.2. Plant Materials

The barks of *Nauclea officinalis* from Hutan Simpan Mersing, Johor were collected by a phytochemical group of the Department of Chemistry, Faculty of Science, Universiti Malaya. The botanical identification was conducted by the botanist, Mr. Teo Leong Eng. The voucher specimen (KL 4745) of the plant was deposited at the Herbarium of the Department of Chemistry, Faculty of Science, Universiti Malaya, Kuala Lumpur, Malaysia.

2.3. Extraction, Isolation and Purification of Compound

The extraction procedure for 1.5 kg of dried and grounded bark of *Nauclea officinalis* was the same as previously described [18,19]. An amount of 6.2 g of CH₂Cl₂ extract was obtained. The CH₂Cl₂ extract was then subjected to column chromatography over silica gel using CH₂Cl₂ and MeOH solvent (100:0, 99:1, 98:2, 97:3, 96:4, 95:5, 94:6, 90:10, 83:17, and 75:25 v/v) and twenty fractions were finally obtained. Further purification from fraction 6 by PTLC yielded nauclediol (8.2 mg, CH₂Cl₂:MeOH; 97:3 v/v saturated with NH₄OH). The structure of nauclediol was elucidated using various spectroscopic methods such as NMR, UV, IR and LCMS-IT-TOF.

2.4. Cholinesterase Enzyme Inhibitory Activity

Naucediol was evaluated for its enzyme inhibition potential against acetylcholinesterase from *Torpedo californica* (TcAChE) and butyrylcholinesterase from *homo sapien* (hBChE). Cholinesterase inhibition was conducted using the Ellman's calorimetry method as described previously [20]. In the 96-well plate, buffer solution, DTNB (Ellman's reagent), ACTI/BUCL and naucediol was added in ascending concentration across the row. 1% DMSO was added as the control for this experiment. Lastly, cholinesterase enzyme was added to the assigned enzymatic columns. The absorbance of the plate was then measured using a spectrophotometer at a wavelength of 412 nm for 30 minutes after the addition of enzymes. Each test was conducted in triplicate to ensure the consistency of the results.

2.5. Molecular Docking

Molecular docking was carried out following the method as described by Abdul Wahab et al [21]. Briefly, molecular docking of naucediol was performed using Autodock 3.0.5 along with AutoDockTools (ADT) [22]. Hyperchem 8 was used to build the 3D-crystal structure of the naucediol and the structure was subjected to energy minimization with a convergence criterion of 0.05 kcal/(molÅ). The three dimensional crystal structures of AChE from *Torpedo californica* (TcAChE) (PDB ID: 1W6R) [23] and BChE from *Homo sapiens* (hBChE) (PDB ID: 2WIJ) [24] were retrieved from the Protein Data Bank. The proteins were edited using ADT to add hydrogen atoms and remove all the water molecules. Non-polar hydrogens and lone pairs were then merged and each atom was assigned with Gasteiger partial charges. A grid box was generated at the center of the active site gorge with 60×60×60 points and spacing of 0.375 Å. One hundred independent dockings were carried out for each docking experiment with a population size of 150 and 2,500,000 energy evaluations. The best conformation with the lowest docked energy in the most populated cluster was selected. Analysis and visualisation of the conformations from the docking experiments were conducted using Accelrys Discovery Studio 2.5 (Accelrys Inc., San Diego, CA, USA).

2.6. Neuroprotective potential of naucediol on Aβ-(1-42)-induced toxicity on SH-SY5Y cells

2.6.1. Cell culture and cell viability assay

Human neuroblastoma cells (SH-SY5Y) were cultured in a complete culture medium containing DMEM nutrient mixture F-12 (1:1) supplemented with 10 % fetal calf serum, glutamine, and 1 % antibiotics (penicillin-streptomycin), and kept at 37 °C under 5 % CO₂.

Cell viability assay was performed to determine the non-cytotoxic concentration of naucediol in SH-SY5Y cells. Cells were seeded with a cell density of 25,000 cells/well in 96 well plates for 24 h. The cells were then treated with naucediol at the concentration of 1, 2, 5, and 10 μM for 24 h. MTT assay was used to assess cell viability after drug treatment. In brief, 20 μl of the MTT solution (5 mg/mL) was added to each well and incubated at 37 °C for 4 hours. 100 μl of DMSO was added to lyse the cells after the removal of the

supernatant in each well. The amount of formazan generated was quantified using a microplate reader (SpectraMax ID3, USA) at an absorbance of 595 nm. All experiments were carried out 3 times.

2.6.2. Neuroprotective Assay Against Beta Amyloid Induced Toxicity

A β -(1-42) oligomers were prepared according to the protocol of Huang et al [25] with some modifications. Briefly, lyophilized A β -(1-42) powder was initially dissolved to 1.0 mM in hexafluoro-2-isopropanol (HFIP) and incubated at room temperature for 30 minutes. The solution was ensured to be clear and colourless. The HFIP was allowed to evaporate in the open tubes overnight in the fume hood. A thin clear film was formed at the bottom of the tube. The film was initially dissolved in DMSO and subsequently adjusted to 13 μ M in DMEM/Hams F-12 media containing 1% Pen/strep and 1% FBS. The solution was incubated at 37 °C under 5 % CO₂.

The MTT assay was used to determine the protection of naucleliol toward SH-SY5Y cells against A β -(1-42) aggregate toxicity. In a 96-well plate, 25,000 cells/well were seeded and incubated overnight. Cells were treated with naucleliol at the concentration of 0.1, 1, 5, and 10 μ M for 24 h. A β -(1-42) aggregates were added to the wells and incubated for another 24 h. 20 μ l of the MTT solution (5 mg/mL) was added to each well and incubated at 37 °C for 4 h. 100 μ l of DMSO was added to lyse the cells after removal of the supernatant in each well. The amount of formazan generated was quantified using a microplate reader (SpectraMax ID3, USA) at an absorbance of 595 nm. All experiments were carried out in triplicate.

2.7. *Anti-Neuroinflammatory Effect of Naucleliol on LPS-Induced Neuro-Inflammation in BV2 Cells*

2.7.1. Cell Culture and Cell Viability Assay

C57/BL6 microglial cells (BV2) were cultured in a complete culture medium containing DMEM supplemented with 10 % fetal calf serum, glutamine, and 1 % antibiotics (penicillin-streptomycin), and kept at 37 °C under 5 % CO₂.

Cell viability assay was performed to determine the non-cytotoxic concentration of naucleliol in BV2 cells. Cells were seeded with a cell density of 20,000 cells/well in 96 well plates for 24 h. The cells were then treated with naucleliol at the concentration of 0.625, 1.25, 2.5, 5, and 10 μ M for 24 h. MTT assay was used to assess cell viability after drug treatment. In brief, 20 μ l of the MTT solution (5 mg/mL) was added to each well and incubated at 37 °C for 4 h. 100 μ l of DMSO was added to lyse the cells after removal of the supernatant in each well. The amount of formazan generated was quantified using a microplate reader (SpectraMax ID3, USA) at an absorbance of 595 nm. All experiments were carried out in triplicate.

2.7.2. Neuroprotective Assay Against LPS-Induced Inflammation

In a 96-well plate, 20,000 cells/well were seeded and incubated overnight. Cells were treated with naucediol at the concentration of 0.0625, 0.125, 0.25, and 0.5 μM for 24 h. LPS (1 $\mu\text{g/ml}$) were added to the wells and incubated for another 24 h. A second 96-well plate was used for the measurement of nitrite oxide. Sulfanilamide and NED solutions were equilibrated to room temperature for 30 min before use. 50 μl of the solution was transferred from the first plate to the second plate. Then, 50 μl of sulfanilamide solution was added to all wells in the second plate and incubated for 5 min. 50 μl of NED solution was subsequently added and incubated for another 5 min. The plate was then read at the absorbance of 540 nm using a microplate reader (SpectraMax ID3, USA). All experiments were carried out in triplicate. The absorbance was converted into a percentage of nitrite to determine the anti-inflammatory effects of naucediol.

2.7.3. Statistical Analysis

Data is analysed using R programming. Data are expressed as mean \pm standard deviation. Differences between groups are analysed using one-way ANOVA followed by Student's *t*-test for MTT assay and nitrite production. A *p*-value less than 0.05 was considered statistically significant.

3. Results and discussion

3.1. Structural Elucidation of Naucediol

Naucediol (Figure 1) was isolated as a brownish amorphous solid. The LCMS-IT-TOF spectrum showed a pseudomolecular ion peak $[\text{M}+\text{Na}]^+$ at m/z 359.1275 (calc. 359.1372), corresponding to the molecular formula of $\text{C}_{20}\text{H}_{20}\text{N}_2\text{O}_3$. UV spectrum of naucediol demonstrated strong absorptions at 374, 308, 277, 256 and 220 nm. In the IR spectrum, an absorption band at 1643 cm^{-1} was observed indicative of a corynanthe type of indole alkaloid with an $\text{N}_4\text{-C=O}$ amide group [26,27]. In addition, a broad hydroxyl absorption band appeared at 3401 cm^{-1} suggesting the presence of hydrogen bonded OH group [27].

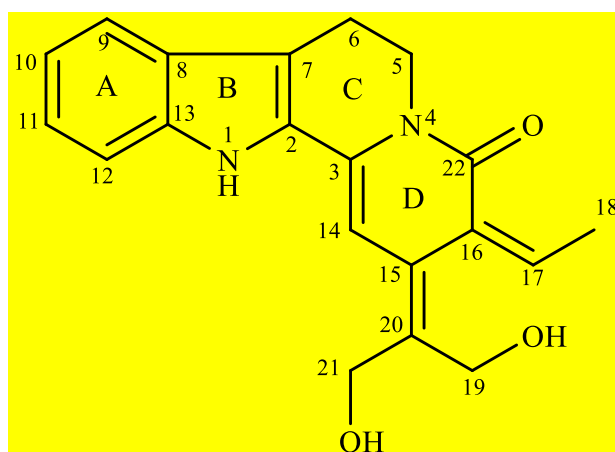


Figure 1. Structure of naucediol.

In the $^1\text{H-NMR}$ spectrum (Table 1), the presence of four aromatic protons signals at the downfield region and a $-\text{CH}_2-\text{CH}_2-\text{N}-$ group were observed, indicating the existence of a tetrahydro- β -carboline skeleton [10,27]. Two of the four aromatic protons in ring A appeared as doublets at δ_{H} 7.53 and 7.37, corresponding to H-9 (1H, *d*, $J = 7.8$ Hz) and H-12 (1H, *d*, $J = 7.8$ Hz), respectively. The other two protons, H-10 (δ_{H} 7.04, 1H, *t*, $J = 7.8$ Hz) and H-11 (δ_{H} 7.19, 1H, *t*, $J = 7.8$ Hz), appeared as triplets. Besides, the COSY spectrum also showed the correlations between the four aromatic protons; H-9 with H-10, H-10 with H-11 and H-11 with H-12 (Figure 2). In addition, two sets of triplet signals which appeared at δ_{H} 4.33 (2H, *t*, $J = 6.9$ Hz) and δ_{H} 3.06 (2H, *t*, $J = 6.9$ Hz) are attributable to methylene protons, H₂-5 and H₂-6 respectively. H-14 of ring D appeared as a singlet at δ_{H} 7.00 indicating the presence of neighbouring quaternary carbons, C-3 (δ_{C} 135.6) and C-15 (δ_{C} 141.2). Furthermore, the presence of downfield quartet at δ_{H} 6.46 (1H, *q*, $J = 6.9$ Hz, H-17) coupled with an upfield doublet at δ_{H} 1.86 (3H, *d*, $J = 6.9$ Hz, H₃-18) implied the presence of a trisubstituted olefin group. Two downfield singlets were observed at δ_{H} 4.45 (2H, *s*, H₂-19) and 4.55 (2H, *s*, H₂-21) which correlated with the carbon signals at δ_{C} 64.1 (C-19) and δ_{C} 64.3 (C-21), respectively in HSQC spectrum, suggesting the existence of two hydroxyl groups (a diol).

Table 1. $^1\text{H-NMR}$ (400 MHz) and $^{13}\text{C-NMR}$ (100 MHz) Spectral Data of naucediol in MeOD.

Position	^1H , δ_{H} (multiplicity, J in Hz)	^{13}C (δ_{C})
2	-	127.5
3	-	135.6
5	4.33 (<i>t</i> , 6.9)	40.5
6	3.06 (<i>t</i> , 6.9)	19.0
7	-	113.0
8	-	125.7
9	7.53 (<i>d</i> , 7.8)	118.9
10	7.04 (<i>t</i> , 7.8)	119.6
11	7.19 (<i>t</i> , 7.8)	124.0
12	7.37 (<i>d</i> , 7.8)	111.3
13	-	138.6
14	7.00 (<i>s</i>)	95.5
15	-	141.2
16	-	120.0
17	6.46 (<i>q</i> , 6.9)	123.8
18	1.86 (<i>d</i> , 6.9)	12.2
19	4.45 (<i>s</i>)	64.1
20	-	129.2
21	4.55 (<i>s</i>)	64.3
22	-	160.9

As indicated in the ^{13}C -NMR and DEPT-135 spectra, naucedliol has a total of twenty carbon signals comprising one methyl, one carbonyl, four methylenes, six methines and eight quaternary carbons. The signal of a carbonyl carbon was observed at δ_{c} 160.9 (C-22). HMBC spectrum showed correlation of H₂-19 and H₂-21 with C-20 (δ_{c} 129.2) indicating the connectivity of the two methylenes with quaternary carbon C-20 as shown in Figure 2. Besides, HMBC correlations between H₃-18 and C-16 (δ_{c} 120.0), H-19 and C-15, H-21 and C-15 were observed, thus supporting the connectivity of trisubstituted olefin group and propane-1,3-diol group to ring D through C-16 and C-15, respectively. The COSY spectrum revealed the correlation peaks between H₂-5 and H₂-6 and H₃-18 and H-17 indicating the respective protons are coupled with each other (Figure 2).

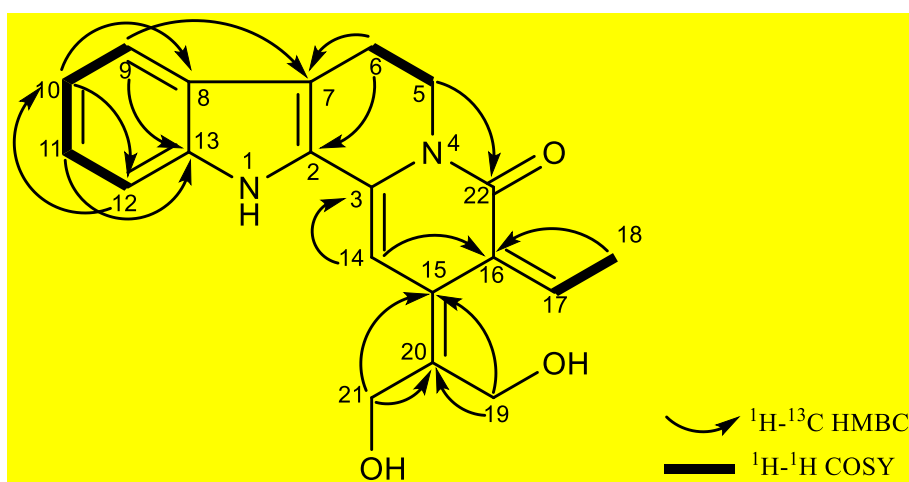


Figure 2. ^1H - ^1H COSY and selected ^1H - ^{13}C HMBC correlations of naucedliol.

Based on the aforementioned and extensive analysis of all spectral data, the structure of naucedliol was established and it is identified as a new corynanthe type of monoterpene indole alkaloid. The biogenetic precursor of naucedliol would be strictosidine. Strictosidine could undergo cleavage of glycoside to strictosidine aglycone followed by cleavage of ring D to form dialdehyde intermediate. Subsequently, a series of rearrangement could lead to the formation of 21-oxogeissoschizine followed by dehydration to form naucedliol as shown in Figure 3.

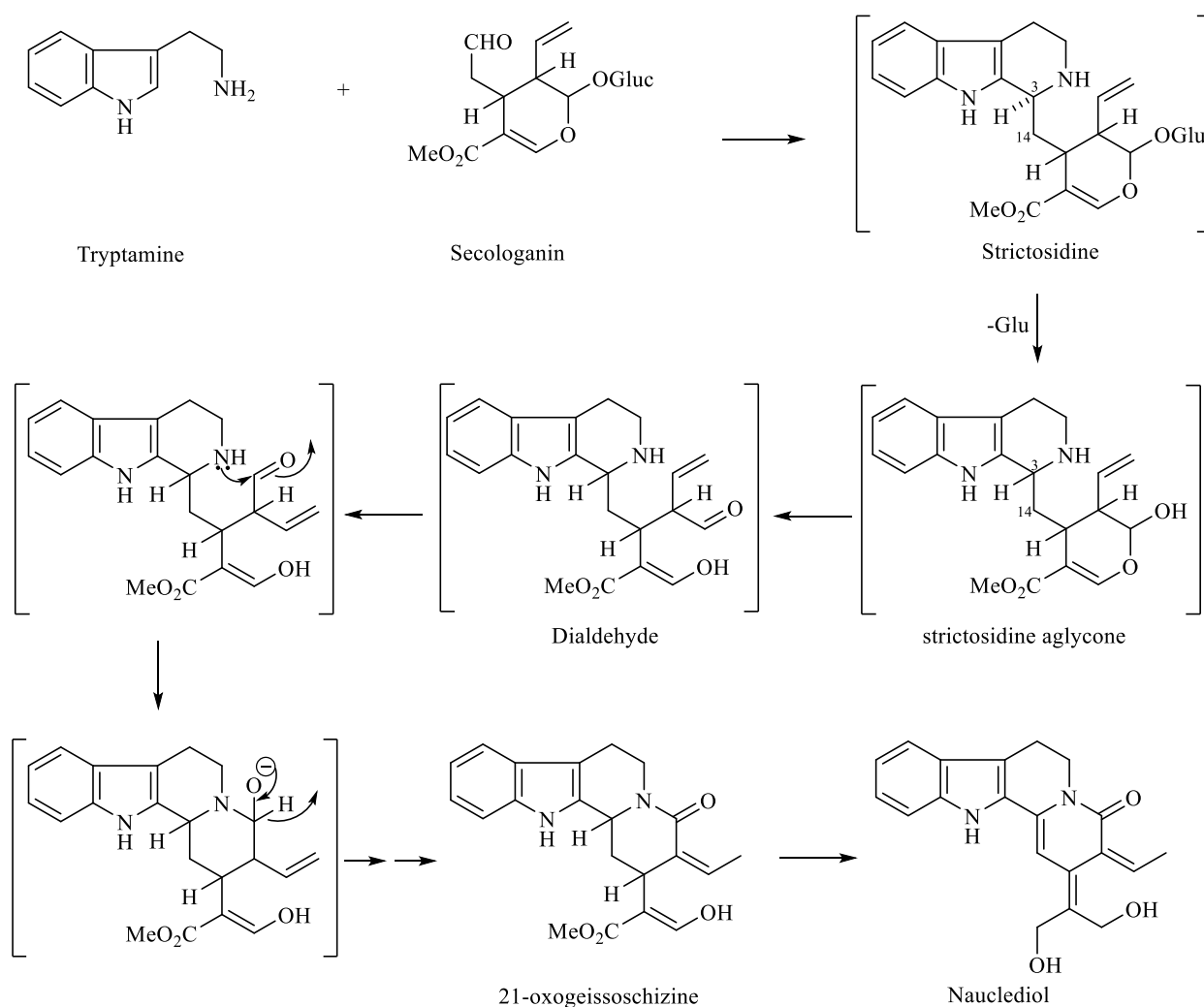


Figure 3. A proposed biogenesis process of naucedliol.

3.2. Cholinesterase Inhibition of Naucedliol

Cholinesterase inhibitors (ChEIs) are the first and most commonly recognized treatment strategy for AD. It works by reducing the metabolism of cholinergic neurotransmitter, acetylcholine released from the cholinergic neurons hence increasing synaptic levels of ACh and BCh [28]. In this study, naucedliol was tested for its inhibitory potential against *TcAChE* and *hBChE*, respectively. Naucedliol showed cholinesterase inhibition activity in both cholinesterase enzymes with an IC_{50} values of 15.429 and 8.756 μM with two-fold more selective toward *hBChE* inhibition (Figure 4). Furthermore, naucedliol was three times more potent as an inhibitor of *BChE* compared to galanthamine (standard or drug) with reported IC_{50} value of 28.29 μM [19].

227

228

229

230

231

232

233

234

235

236

237

238

239

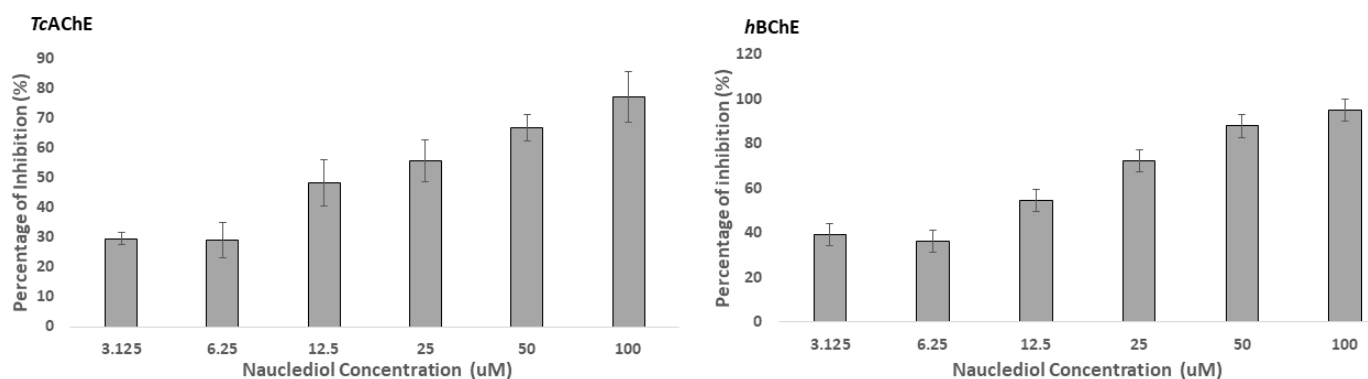


Figure 4. Cholinesterase inhibition of naucediol.

The mode of inhibition was determined by means of Lineweaver-burk plot. Figure 5 shows the kinetic plots of naucediol and the mode of inhibition of naucediol for both enzymes were identified to be mixed types inhibition. The K_i values of naucediol were 25.287 and 20.401 for both TcAChE and hBChE, respectively (Appendix S1), which is well correlated with IC_{50} value obtained. Secondary plots (K_{is}) for naucediol were presented as mixed type inhibitors that could bind in the free enzyme (K_i) and inhibit substrate bound-enzymes. By comparing the potency of the naucediol in inhibiting cholinesterase enzymes, the K_i and K_{is} of the naucediol for hBChE (20.40 and 45 μM) was stronger than TcAChE (25.287 and 36.51 μM) as well as lower K_i value indicating naucediol bind more firmly to the free cholinesterase enzyme than the enzyme-substrate complex.

It is worth noting that all drugs available in the market are AChE inhibitors and compounds acting on BChE might be an interesting target for anti-cholinesterase discovery. Naucediol appeared to be a mixed mode inhibitor of both AChE and BChE.

By comparing with the cholinesterase inhibitory activities of other indole alkaloids that isolated from *N. officinalis* [19], a brief structure-activity relationship studies can be conducted. Angustidine, angustine, angustoline and naucline are also corynanthe type of indole alkaloids [19] with the same precursors as naucediol. According to the proposed biogenesis pathway, the difference between naucediol and the four known indole alkaloids is starts after the formation of strictosidine. Rotation at C-14 of strictosidine is needed to form strictosidine lactam followed by the formation of the four known indole alkaloids. On the other hand, formation of naucediol does not require the rotation at C-14 of strictosidine but involve a ring opening in strictosidine aglycone. Hence, the four known indole alkaloids possess ring E (pyridine or pyran ring) but naucediol does not. Based on the previously reported data, angustidine, angustine, angustoline and naucline exhibited moderate to weak AChE inhibition with angustidine having the lowest IC_{50} values (21.72 μM) [19], In comparison with the four known indole alkaloids, naucediol possess better inhibitory effect towards AChE. It was suggested that the potency of naucediol on AChE inhibition may due to the presence of ring-opened system in ring E and the two hydroxyl

groups. For BChE, angustidine and angustine ($IC_{50} = 1.03$ and 4.98 , respectively) [19] showed better inhibitory effect compared to nauclediol. However, nauclediol was 2.5 and 4 times more potent than angustoline and naucline, respectively in which angustoline has only one hydroxyl group in its structure while naucline has a pyran ring instead of pyridine ring (ring E). Based on structure-relationship studies, the potency in inhibiting BChE may be contributed by the presence of pyridine ring and the potency could be increased if having two hydroxyl groups.

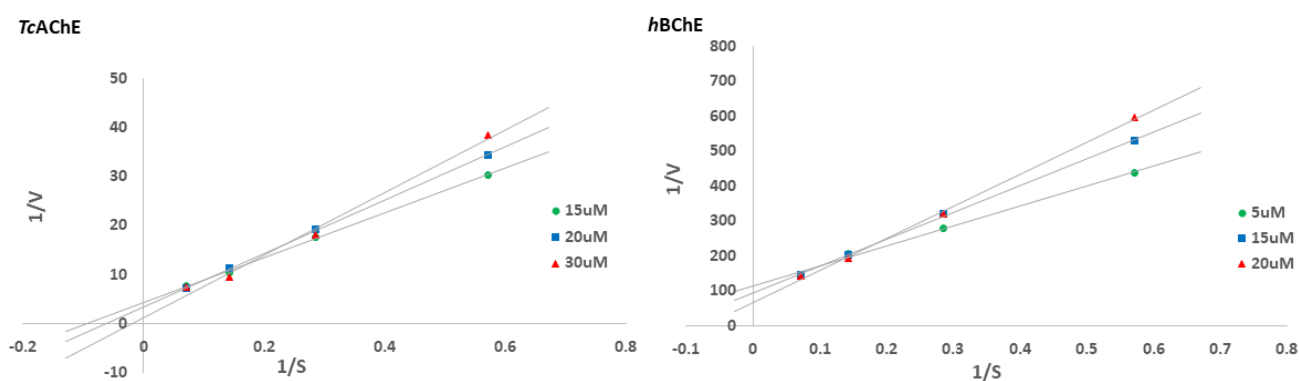


Figure 5. Lineweaver-Burk plots of nauclediol.

3.3. Molecular Docking of Nauclediol

Since nauclediol is potent in inhibiting both enzymes, molecular docking analysis was carried out in order to understand its binding interaction with the enzymes. The results revealed that nauclediol docked well in the catalytic triad and choline binding site of *TcAChE* (Table 2). The hydroxyl group of C-19 formed a hydrogen bond with His 440 at a distance of 2.60 \AA in the catalytic triad (Table 2). Catalytic triad serves as the active site of the enzyme where acetylcholine, the substrate, is hydrolysed into choline and acetate [21]. Besides, hydrogen bond and hydrophobic interaction were observed between the compound and the amino acid residues in the choline binding site which anchored this compound to the *TcAChE* active site gorge (Figure 6). Oxygen atom of the carbonyl group C-22 interacted with Tyr 130 through hydrogen bond at a distance of 2.26 \AA while the ring B and D of the compound formed π - π stacking interaction with Trp 84. For *hBChE*, nauclediol also bound with amino acid residues of the catalytic triad and choline binding site with hydrophobic interaction (Table 2). A π - π stacking interaction was observed between the indole ring of nauclediol with His 438 from the active site of *hBChE* as shown in Figure 7. In addition, a π - σ interaction was observed between Trp 82 with C-17 of nauclediol. This finding was in agreement with the mode of inhibition of nauclediol; mixed type of inhibition, which indicated that the compound was able to bind to the active site and allosteric site (choline binding site) of both enzymes.

Table 2. Binding interaction data for naucleliol with amino acid residues of *TcAChE* and *hBChE*.

302

Ligand/ Compound	Enzyme	Binding Energy (kcal/mol)	Number of conformations in the cluster	Interacting site	Residue	Type of Interaction	Distance (Å)	Ligand Interacting
Naucleliol	<i>TcAChE</i>	-13.01	64	Catalytic triad	His 440	Hydrogen	2.60	Hydroxyl group at C-19
				Choline binding site	Trp 84 Tyr 130	Hydrophobic Hydrogen	- 2.26	Ring B and D Oxygen atom of the carbonyl group C-22
	<i>hBChE</i>	-12.19	60	Catalytic triad	His 438	Hydrophobic	-	Ring A and B
				Choline binding site	Trp 82	Hydrophobic	-	C-17

303

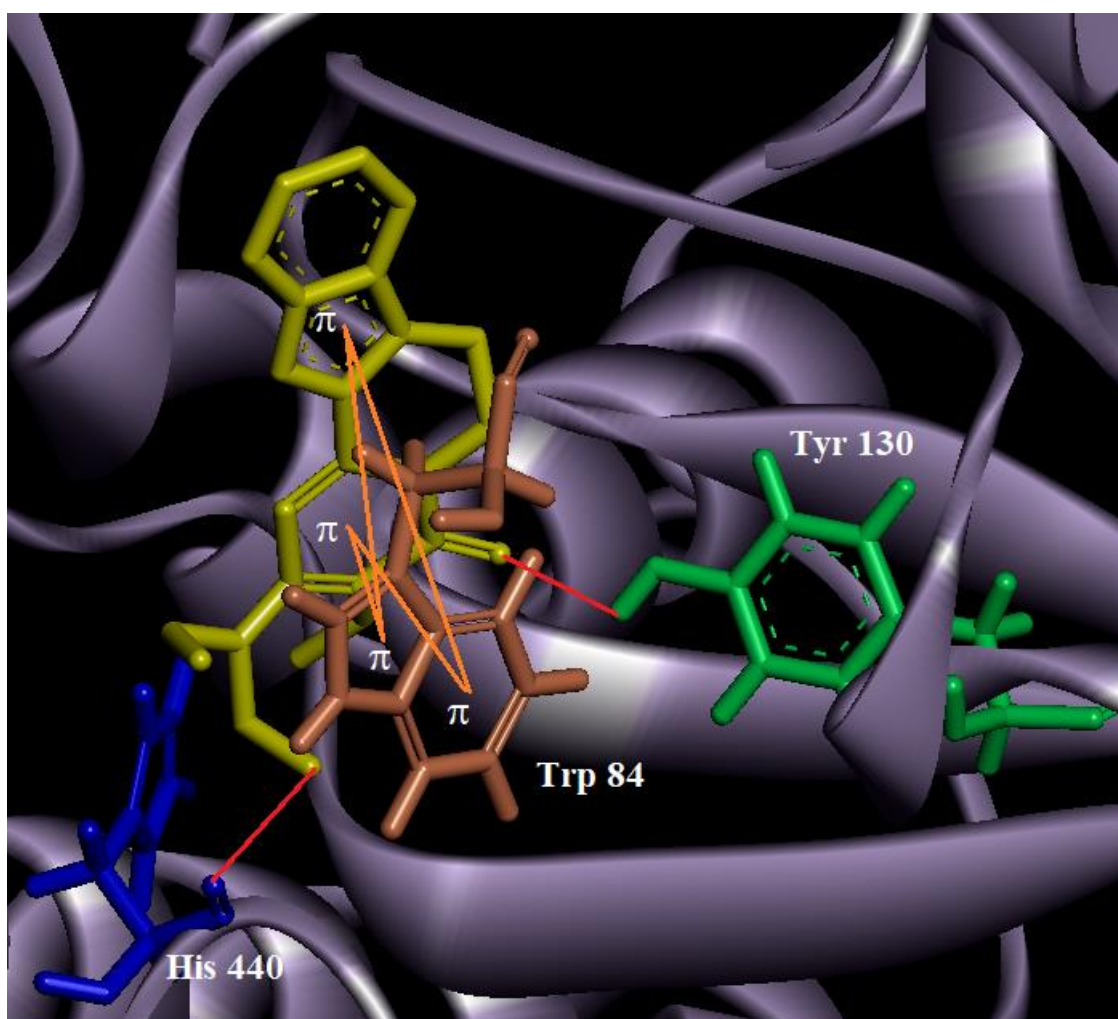


Figure 6. Binding interaction of naucediol (in yellow) with amino acid residues of *TcAChE*. The hydrogen bond between the ligand and amino acid residues are shown in red line.

304

305

306

307

308

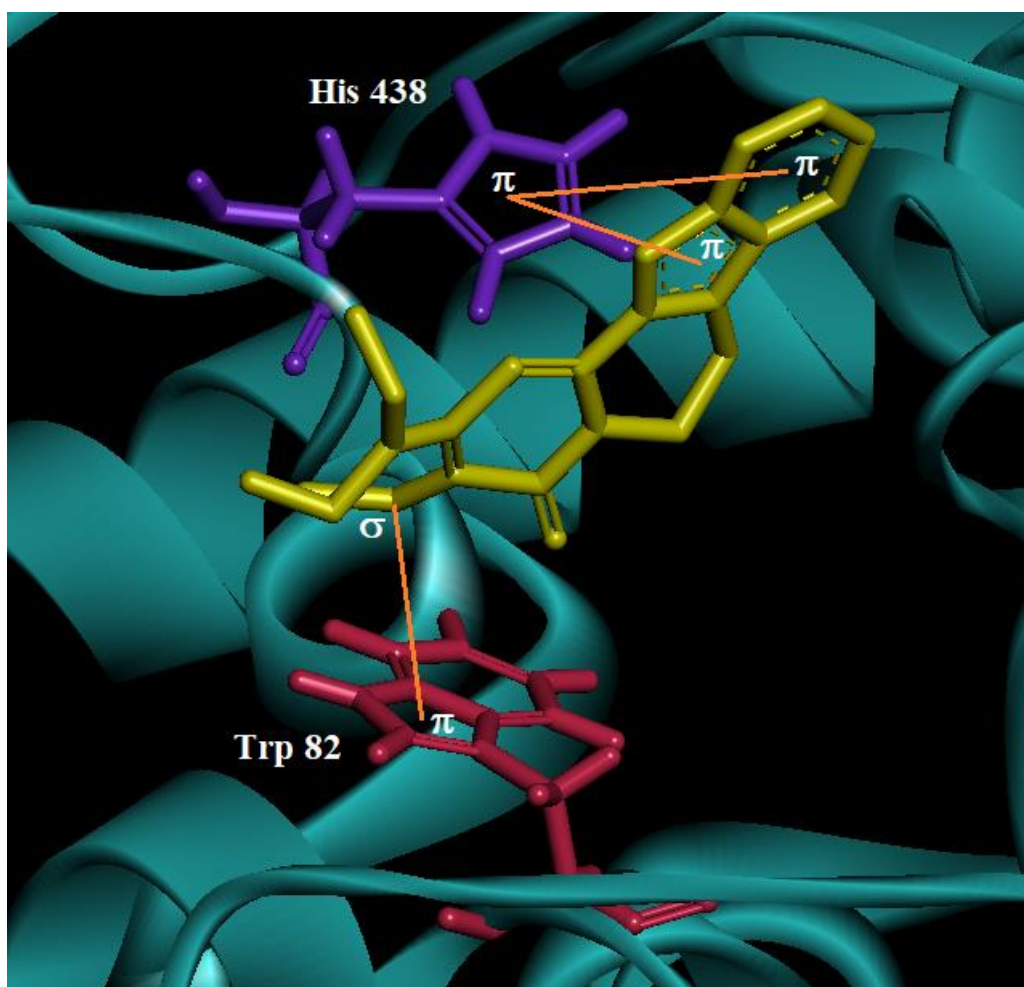


Figure 7. Binding interaction of naucedliol (in yellow) with amino acid residues of *hBChE*.

3.4. Naucedliol Reduces $A\beta$ -(1-42)-Induced Toxicity on SH-SY5Y Cells

As illustrated in Figure 8A, naucedliol had no cytotoxic effect on SH-SY5Y cells from 1 to 10 μM . Further, the cells were pretreated with 1 to 10 μM of naucedliol followed by $A\beta$ -(1-42) aggregates. Figure 8B shows that 13 μM $A\beta$ -(1-42) aggregates significantly reduced cell viability to $54.5 \pm 6.52\%$ compared to the untreated cells. The cell viability of neuroblastoma SH-SY5Y cells was increased by 33.28 to 64.87% at the tested concentrations (0.1 to 10 μM) compared to cells treated with $A\beta$ -(1-42) aggregates alone. Overall, our study showed that naucedliol protected neuroblastoma SH-SY5Y cells against $A\beta$ -(1-42) induced cytotoxicity.

309

310

311

312

313

314

315

316

317

318

319

320

321

322

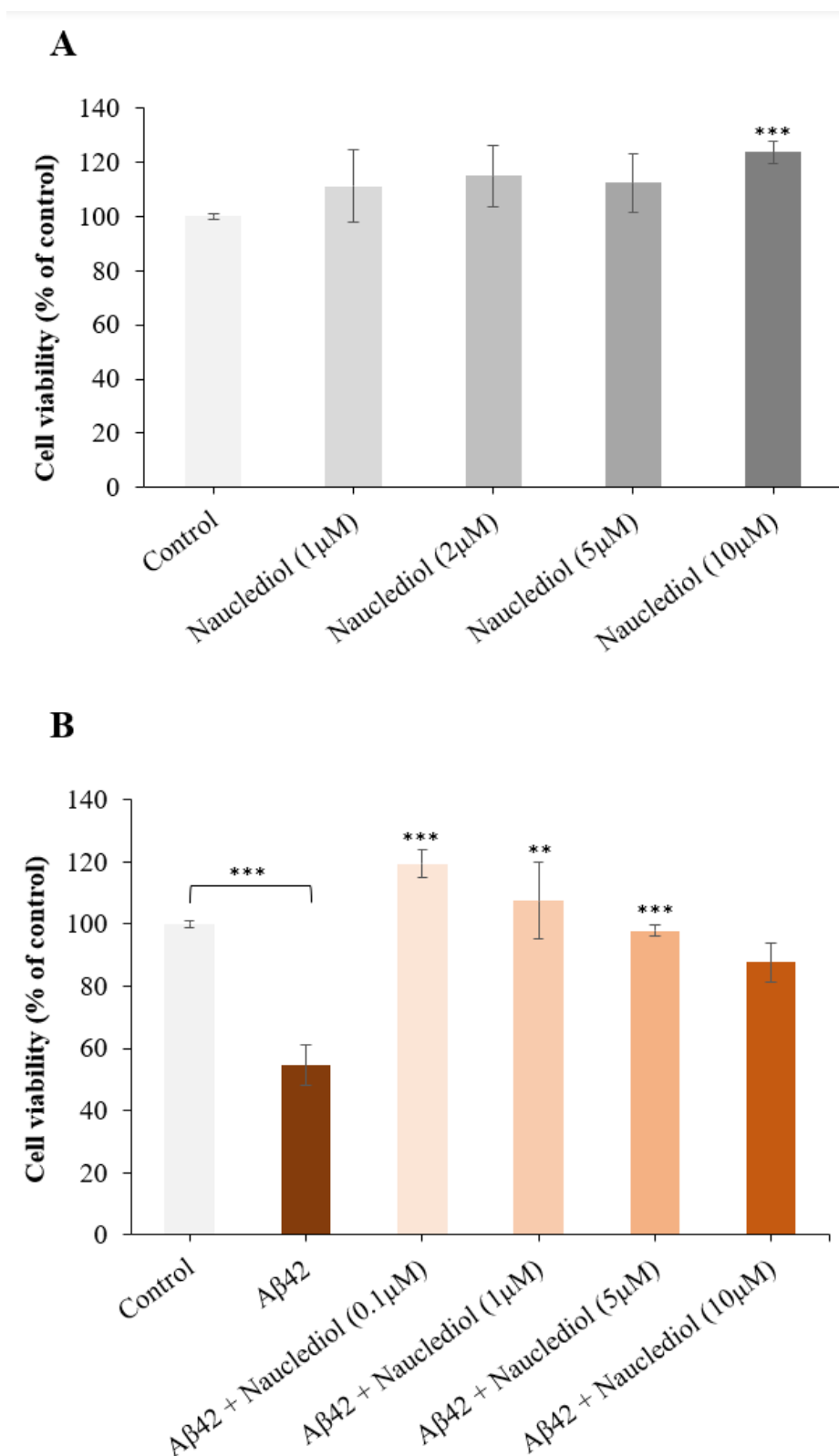


Figure 8. Neuroprotective activity of naucleliol on SH-SY5Y cells. (A) Cells were treated with various doses of naucleliol for 24 h. (B) Cells were pre-treated with non-detrimental concentrations of naucleliol for 24 h before exposure to 13 μM Aβ-(1-42) aggregates for 24 h. Data are expressed as mean ± standard deviation of three independent experiments, statistical significance was performed by one-way ANOVA followed by Student's t-test; *, **, ***, and **** indicate significant statistical differences between treated and untreated control cells or versus Aβ-(1-42) aggregates (p < 0.05).

323

324

325

326

327

328

3.5. Naucleliol Reduces LPS-Induced Neuroinflammation in BV2 Cells

Naucleliol was tested for its cytotoxic effect on BV2 cells at 1.25 to 10 μM . Figure 9 shows BV2 cell viabilities upon exposure to naucleliol. Treated doses at 1.25 to 10 μM were cytotoxic towards BV2 cells from 9.28 to 22.7% when compared to untreated cells. Non-toxic doses at 0.0625 to 0.5 μM were used for further experiments. Naucleliol demonstrated a statistically significant reduction in nitrite at the doses of 0.25 to 0.5 μM .

In this test, we sought to evaluate whether naucleliol could reduce the elevated levels of the nitric oxide production of the LPS-induced inflammation in BV2 cells. Several studies have shown the relationship between nitric oxide and the pathogenesis of AD such as neuronal death and S-nitrosylation of cellular components [29]. In addition, in postmortem brain tissues from AD patients, $\text{A}\beta$ plaques are strongly associated with reactive microglia and nitric oxide production from activated microglia [30].

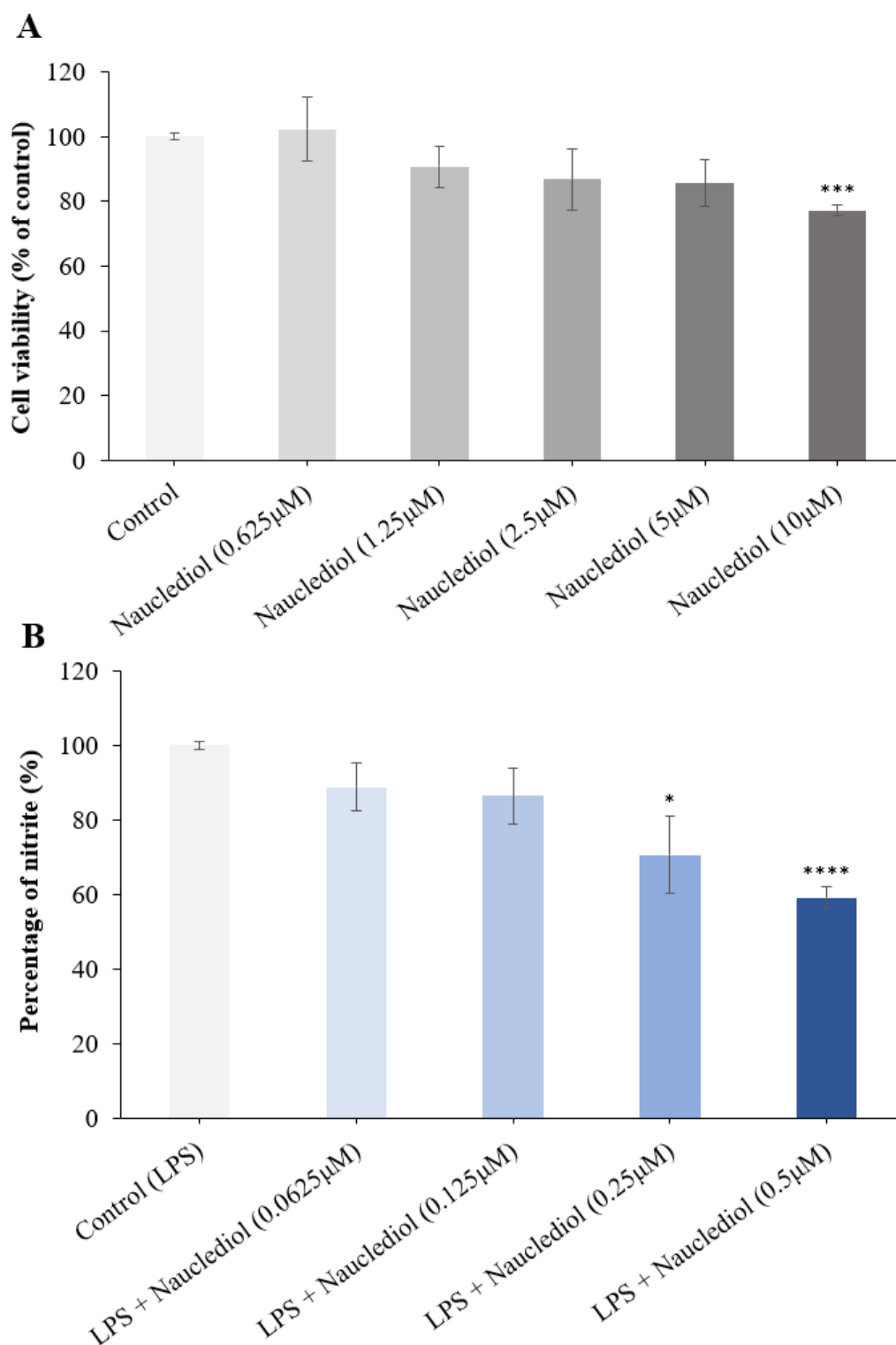


Figure 9. Anti-neuroinflammation activity of naucleliol. (A) BV2 cells were treated with various doses of naucleliol for 24 h. (B) BV2 cells were pre-treated with non-detrimental concentrations of naucleliol for 24 h before exposure to LPS (1 µg/ml) for 24 h. Data are expressed as mean ± standard deviation of three independent experiments, statistical significance was performed by one-way ANOVA followed by Student's t-test; *, **, ***, and **** indicate significant statistical differences between treated and untreated control cells or versus LPS (p < 0.05).

341

342

343

344

345

346

5. Conclusions

In conclusion, the present study has yielded a new monoterpenoid indole alkaloid, nauclediol from *Nauclea officinalis* which is a dual cholinesterase inhibitor with two-fold more selective against butyrylcholinesterase enzyme. Upon a molar basis comparison with galantamine; drug or medication used in treatment of Alzheimer disease, nauclediol was three times more potent in inhibiting BChE. Besides, lineweaver burk plot and molecular docking showed that nauclediol is a mixed inhibitor. In addition, nauclediol was significantly protected cells against beta amyloid induced toxicity and neuroinflammation at submicromolar levels. Overall, the findings in this study are worth further investigation for its potential in other neurodegenerative diseases related assay.

Author Contributions: Conceptualization, S.Y.L., K.Y.K. and K.A.; Methodology, S.Y.L., K.Y.K., H.H., M.L. and K.A.; Investigation, S.Y.L. and K.Y.K.; Data Analysis, S.Y.L., M.W.Q, T.H.Y. K.Y.K. H.H., M.L. and K.A.; Writing – Original Draft Preparation, S.Y.L., M.W.Q, T.H.Y. K.Y.K.; Writing – Review and Editing, S.Y.L., M.W.Q, T.H.Y. K.Y.K. H.H., M.L. and K.A.; Project Administration, S.Y.L., K.Y.K., M.L. and K.A. All authors have read and agreed to the published version of the manuscript.

Funding: This work was supported by Universiti Malaya Research Grant (RK011-2020).

Institutional Review Board Statement: Not applicable.

Informed Consent Statement: Not applicable.

Data Availability Statement: Not applicable.

Acknowledgement: The authors sincerely thank D. M. Nor and Rafly bin Syamsir (Universiti Malaya) for the collection of plant material and Mr. Teo Leong Eng for the botanical identification. The authors would also like to thank the International French Malaysia Natural Product Laboratory (IFM-NatProLab) between CNRS-ICSN, the French Embassy in Malaysia and Universiti Malaya for the collaborative work.

Conflicts of Interest: The authors declare no conflict of interest.

References

1. Wee, S.A.; Nhu, D.T.; Khaw, Y.K.; Tang, S.K.; Yeong, Y.K. Linking Diabetes to Alzheimer's Disease: Potential Roles of Glucose Metabolism and Alpha-Glucosidase. *Current Neuropharmacology* **2023**, *21*, 1-13, doi:http://dx.doi.org/10.2174/1570159X21999221111102343. 376-379
2. Mukherjee, P.K.; Kumar, V.; Mal, M.; Houghton, P.J. Acetylcholinesterase inhibitors from plants. *Phytomedicine* **2007**, *14*, 289-300, doi:https://doi.org/10.1016/j.phymed.2007.02.002. 380-381
3. Iqubal, A.; Rahman, S.O.; Ahmed, M.; Bansal, P.; Haider, M.R.; Iqubal, M.K.; Najmi, A.K.; Pottou, F.H.; Haque, S.E. Current Quest in Natural Bioactive Compounds for Alzheimer's Disease: Multi-Targeted-Designed-Ligand Based Approach with Preclinical and Clinical Based Evidence. *Curr Drug Targets* **2021**, *22*, 685-720, doi:10.2174/1389450121999201209201004. 382-385
4. Kong, Y.R.; Tay, K.C.; Su, Y.X.; Wong, C.K.; Tan, W.N.; Khaw, K.Y. Potential of Naturally Derived Alkaloids as Multi-Targeted Therapeutic Agents for Neurodegenerative Diseases. *Molecules* **2021**, *26*, 728. 386-387
5. Kong, Y.R.; Jong, Y.X.; Balakrishnan, M.; Bok, Z.K.; Weng, J.K.K.; Tay, K.C.; Goh, B.H.; Ong, Y.S.; Chan, K.G.; Lee, L.H.; et al. Beneficial Role of Carica papaya Extracts and Phytochemicals on Oxidative Stress and Related Diseases: A Mini Review. *Biology* **2021**, *10*, 287. 388-390
6. Williams, D.H.; Stone, M.J.; Hauck, P.R.; Rahman, S.K. Why Are Secondary Metabolites (Natural Products) Biosynthesized? *J. Nat. Prod.* **1989**, *52*, 1189-1208, doi:10.1021/np50066a001. 391-392
7. Croteau, R.; Kutchan, T.M.; Lewis, N.G. *Natural products (secondary metabolites)*; American Society of Plant Physiologists: 2000; Volume 24, pp. 1250-1318. 393-394
8. Calixto, J.B.; Otuki, M.F.; Santos, A.R.S. Anti-Inflammatory Compounds of Plant Origin. Part I. Action on Arachidonic Acid Pathway, Nitric Oxide and Nuclear Factor κ B (NF- κ B). *Planta Med.* **2003**, *69*, 973-983, doi:10.1055/s-2003-45141. 395-397
9. Mcconnell, O.J.; Saucy, G.; Jacobs, R. Use for topsentin compounds and pharmaceutical compositions containing same. **5290777**, 1994. 398-399
10. Sun, J.Y.; Lou, H.X.; Dai, S.J.; Xu, H.; Zhao, F.; Liu, K. Indole alkaloids from *Nauclea officinalis* with weak antimalarial activity. *Phytochemistry* **2008**, *69*, 1405-1410, doi:http://dx.doi.org/10.1016/j.phytochem.2008.01.008. 400-401
11. Sun, J.Y.; Lou, H.X.; Xu, H.; Dai, S.J.; Liu, K. Two new indole alkaloids from *Nauclea officinalis*. *Chinese Chemical Letters* **2007**, *18*, 1084-1086. 402-403
12. Su, K.; Gong, M.; Zhou, J.; Deng, S. Study of Chemical Composition of *Nauclea Officinalis* Leaves. *International Journal of Chemistry* **2009**, *1*, 77-81. 404-405
13. Song, L.-L.; Mu, Y.-L.; Zhang, H.-C.; Wu, G.-Y.; Sun, J.-Y. A new indole alkaloid with anti-inflammatory from the branches of *Nauclea officinalis*. *Natural Product Research* **2018**, *34*, 2283-2288, doi:https://doi.org/10.1080/14786419.2018.1536130. 406-408

14. Song, S.; Liu, P.; Wang, L.; Li, D.; Fan, H.; Chen, D.; Zhao, F. In vitro anti-inflammatory activities of naucleoffeine H as a natural alkaloid from *Nauclea officinalis* Pierr ex Pitard, through inhibition of the iNOS pathway in LPS-activated RAW 264.7 macrophages. *Natural Product Research* **2020**, *34*, 2694-2697, doi:10.1080/14786419.2018.1550765. 409-412
15. Liew, S.Y.; Looi, C.Y.; Paydar, M.; Cheah, F.K.; Leong, K.H.; Wong, W.F.; Mustafa, M.R.; Litaudon, M.; Awang, K. Subditine, a New Monoterpenoid Indole Alkaloid from Bark of *Nauclea subdita* (Korth.) Steud. Induces Apoptosis in Human Prostate Cancer Cells. *PLoS ONE* **2014**, *9*, e87286, doi:10.1371/journal.pone.0087286. 413-415
16. Qureshi, A.K.; Mukhtar, M.R.; Hirasawa, Y.; Hosoya, T.; Nugroho, A.E.; Morita, H.; Shirota, O.; Mohamad, K.; Hadi, A.H.A.; Litaudon, M.; et al. Neolamarckines A and B, New Indole Alkaloids from *Neolamarckia cadamba*. *Chemical & Pharmaceutical Bulletin* **2011**, *59*, 291-293. 416-418
17. Mukhtar, M.R.; Osman, N.; Awang, K.; Hazni, H.; Qureshi, A.K.; Hadi, A.H.A.; Zaima, K.; Morita, H.; Litaudon, M. Neonaucline, a New Indole Alkaloid from the Leaves of *Ochreinauclea maingayii* (Hook. f.) Ridsd. (Rubiaceae). *Molecules* **2011**, *17*, 267-274. 419-421
18. Liew, S.Y.; Mukhtar, M.R.; Hadi, A.H.A.; Awang, K.; Mustafa, M.R.; Zaima, K.; Morita, H.; Litaudon, M. Naucline, a New Indole Alkaloid from the Bark of *Nauclea officinalis*. *Molecules* **2012**, *17*, 4028-4036. 422-423
19. Liew, S.Y.; Khaw, K.Y.; Murugaiyah, V.; Looi, C.Y.; Wong, Y.L.; Mustafa, M.R.; Litaudon, M.; Awang, K. Natural indole butyrylcholinesterase inhibitors from *Nauclea officinalis*. *Phytomedicine* **2015**, *22*, 45-48, doi:http://dx.doi.org/10.1016/j.phymed.2014.11.003. 424-426
20. Khaw, K.Y.; Chong, C.W.; Murugaiyah, V. LC-QTOF-MS analysis of xanthone content in different parts of *Garcinia mangostana* and its influence on cholinesterase inhibition. *J Enzyme Inhib Med Chem* **2020**, *35*, 1433-1441, doi:10.1080/14756366.2020.1786819. 427-429
21. Abdul Wahab, S.M.; Sivasothy, Y.; Liew, S.Y.; Litaudon, M.; Mohamad, J.; Awang, K. Natural cholinesterase inhibitors from *Myristica cinnamomea* King. *Bioorganic & Medicinal Chemistry Letters* **2016**, *26*, 3785-3792, doi:https://doi.org/10.1016/j.bmcl.2016.05.046. 430-432
22. Morris, G.M.; Goodsell, D.S.; Halliday, R.S.; Huey, R.; Hart, W.E.; Belew, R.K.; Olson, A.J. Automated docking using a Lamarckian genetic algorithm and an empirical binding free energy function. *Journal of Computational Chemistry* **1998**, *19*, 1639-1662, doi:https://doi.org/10.1002/(SICI)1096-987X(19981115)19:14<1639::AID-JCC10>3.0.CO;2-B. 433-436
23. Greenblatt, H.M.; Guillou, C.; Guénard, D.; Argaman, A.; Botti, S.; Badet, B.; Thal, C.; Silman, I.; Sussman, J.L. The Complex of a Bivalent Derivative of Galanthamine with Torpedo Acetylcholinesterase Displays Drastic Deformation of the Active-Site Gorge: Implications for Structure-Based Drug Design. *Journal of the American Chemical Society* **2004**, *126*, 15405-15411, doi:10.1021/ja0466154. 437-440
24. Carletti, E.; Aurbek, N.; Gillon, E.; Loiodice, M.; Nicolet, Y.; Fontecilla-Camps, J.-C.; Masson, P.; Thiermann, H.; Nachon, F.; Worek, F. Structure-activity analysis of aging and reactivation of human butyrylcholinesterase inhibited by analogues of tabun. *Biochemical Journal* **2009**, *421*, 97-106, doi:10.1042/bj20090091. 441-443

-
25. Chunhui, H.; Dilin, X.; Ke, Z.; Jieyi, S.; Sicheng, Y.; Dapeng, W.; Qinwen, W.; Wei, C. A11-positive β -amyloid Oligomer Preparation and Assessment Using Dot Blotting Analysis. *J Vis Exp* **2018**, doi:10.3791/57592. 444
445
26. Au, T.Y.; Cheung, H.T.; Sternhell, S. New corynanthé alkaloids from *Strychnos angustiflora*. *Journal of the Chemical Society, Perkin Transactions 1* **1973**, 13-16, doi:10.1039/P19730000013. 446
447
27. Shigemori, H.; Kagata, T.; Ishiyama, H.; Morah, F.; Ohsaki, A.; Kobayashi, J.i. Naucleamides A—E, New Monoterpene Indole Alkaloids from *Nauclea latifolia*. *Chemical and Pharmaceutical Bulletin* **2003**, *51*, 58-61, doi:10.1248/cpb.51.58. 448
449
450
28. Cavalli, A.; Bolognesi, M.L.; Minarini, A.; Rosini, M.; Tumiatti, V.; Recanatini, M.; Melchiorre, C. Multi-target-directed ligands to combat neurodegenerative diseases. *J Med Chem* **2008**, *51*, 347-372, doi:10.1021/jm7009364. 451
452
29. Doherty, G.H. Nitric oxide in neurodegeneration: potential benefits of non-steroidal anti-inflammatories. *Neuroscience Bulletin* **2011**, *27*, 366-382, doi:10.1007/s12264-011-1530-6. 453
454
30. Sparrow, J.R. Inducible nitric oxide synthase in the central nervous system. *J Mol Neurosci* **1994**, *5*, 219-229, doi:10.1007/bf02736723. 455
456

Disclaimer/Publisher's Note: The statements, opinions and data contained in all publications are solely those of the individual author(s) and contributor(s) and not of MDPI and/or the editor(s). MDPI and/or the editor(s) disclaim responsibility for any injury to people or property resulting from any ideas, methods, instructions or products referred to in the content. 457
458
459